21st Australasian Fluid Mechanics Conference
Adelaide, Australia
10-13 December 2018

LES of a temporally evolving non-premixed CO/H_2 jet flame involving extinction and re-ignition

H. D. Ranadive[1], B. Savard[1] and E. R. Hawkes[1,2]

[1]School of Mechanical and Manufacturing Engineering
University of New South Wales, NSW 2052, Australia

[2]School of Photovoltaic and Renewable Energy Engineering
University of New South Wales, NSW 2052, Australia

Abstract

Large-eddy simulations (LES) of a temporally evolving non-premixed CO/H_2 jet flame are conducted with a compressible high-order accurate numerical solver. The configuration is challenging due to the presence of significant flame extinction followed by re-ignition. The LES results are assessed by comparing them with previously conducted direct numerical simulations of the same configuration. The sub-grid scale turbulence-chemistry interactions are modelled using a transported probability density function (PDF) approach. The transport equation for the composition PDF is solved using a particle-based Lagrangian solver, that is tightly coupled with the Eulerian solver. The capability of the LES/PDF model to capture the sub-grid turbulence-chemistry interactions, and in particular the extinction and re-ignition phenomenon of this flame is demonstrated by comparing the results with a LES simulation with a well-mixed approximation. A sensitivity study of the PDF model parameters has been conducted to demonstrate the reliability of the model predictions.

Introduction

Numerical simulations of turbulent reacting flows are imperative to the propulsion and power generation industry [24], but accurate predictions are challenging when the turbulent flames involve extinction and re-ignition phenomena that are intricately governed by the small-scale turbulence-chemistry interactions (TCI).

Large-eddy simulations (LES) are a class of such simulations that are conducted by explicitly resolving the large-scale turbulence and employing models for the sub-grid scale (SGS) contributions. In a LES, the modelling of the non-linear chemical source term is challenging because of the dependence of chemical reactions on small-scale mixing [18]. A well-mixed (WM) approximation, in which the sub-grid TCI are ignored, is recommended only for a well-resolved LES [7]. To this end, significant research effort has been invested in the development of SGS combustion models like the flamelet model [19], transported probability density function (PDF) [13] and conditional moment closure (CMC) [16]. In particular, the PDF models have attracted significant attention due to the closed form formulation of the chemical source term and their applicability to a broad range of combustion regimes [11].

Hybrid solvers employed for LES/PDF simulations include an Eulerian (grid-based) solver for the flow and turbulence and a Lagrangian (particle-based) solver for the transported scalars like enthalpy and species mass fractions [13]. The majority of LES/PDF implementations [20, 13, 2, 26] employ first order accurate time integration of the stochastic differential equations (SDE) governing the particle evolution. Wang et al. [22] first presented weak second-order accurate splitting schemes in a low Mach solver formulation, which have not been noted with compressible formulations so far. In the context of spatial discretisation, most LES/PDF solvers use second-order accurate schemes [25, 20, 5], with limited examples having fourth [2] or higher order non-dissipative methods.

In this work, we present the first application of our newly developed solver which features weak second-order time integration of the particle governing equations (using stochastic Runge-Kutta (RK) schemes presented by Wilkie [23]), non-dissipative [1] eight-order accurate central difference spatial discretisation schemes and a fully compressible PDF implementation. Furthermore, the particle solver is tightly coupled with the Eulerian solver at every sub-step of the high-order RK algorithm in order to minimise the splitting errors across the various particle updates like transport, mixing or reaction. This implementation is done in the S3D solver [4], which has been extensively employed for direct numerical simulations (DNS) of turbulent flames [10, 9].

A temporally evolving non-premixed flame involving significant extinction followed by re-ignition has been chosen for the assessment of the current solver. This configuration was first studied with DNS by Hawkes et al. [10] and later used for validation in a low Mach LES/PDF study by Yang et al. [25]. Further we show the importance of using a sub-grid TCI model by comparing the results with a LES/WM simulation that ignores these sub-grid variations. The rest of the paper is organised as follows: the LES models and the numerical schemes are discussed in the forthcoming section. Next, the configuration details are discussed briefly, followed by the results and discussion. The final section concludes the paper with key remarks.

Methodology

Filtered governing equations

The filtered fully-compressible system of equations solved on an Eulerian mesh are given below:

$$\frac{\partial \bar{\rho}}{\partial t} = -\nabla \cdot (\bar{\rho}\tilde{\mathbf{u}}), \tag{1}$$

$$\frac{\partial \bar{\rho}\tilde{\mathbf{u}}}{\partial t} = -\nabla \cdot [\bar{\rho}\tilde{\mathbf{u}}\tilde{\mathbf{u}} + \bar{p}\underline{\delta} - \underline{\tau}], \tag{2}$$

$$\frac{\partial \bar{\rho}\tilde{E}}{\partial t} = -\nabla \cdot \left[\left(\bar{\rho}\tilde{E} + \bar{p}\right)\tilde{\mathbf{u}} + \mathbf{q} - \underline{\tau}\cdot\tilde{u}\right], \tag{3}$$

$$\frac{\partial \bar{\rho}\tilde{Y_\alpha}}{\partial t} = -\nabla \cdot \left[\bar{\rho}\tilde{\mathbf{u}}\tilde{Y_\alpha} + \mathbf{J}_\alpha\right] + \tilde{\dot{\omega}}_\alpha + \tilde{F}_\alpha, \tag{4}$$

where the over-bar ($\bar{\phi}$) denotes a filtered variable and the tilde ($\tilde{\phi}$) denotes a Favre filtered variable ($\overline{\rho\phi}/\bar{\rho}$), ρ is the density, p is the pressure, $\mathbf{u}$ is the velocity, $\underline{\delta}$ is the unit tensor, $\underline{\tau}$ is the viscous and SGS stress tensor, $\mathbf{q}$ is the molecular and SGS heat flux vector and $\tilde{E} = \tilde{\mathbf{u}}\cdot\tilde{\mathbf{u}}/2 + \tilde{h} - \bar{p}/\bar{\rho}$ is the specific total energy (comprised of internal (e) and kinetic energy) with h denoting the gas enthalpy. For each species denoted by $\alpha = 1, 2, ..., N_s$

(N_s is the total number of species), Y_α is its mass fraction, $\mathbf{J}_\alpha$ is its molecular and SGS diffusive flux and $\dot{\omega}_\alpha$ is its chemical source term. The ideal gas assumption is used for the equation of state.

In the case of the TPDF simulations, the term $\tilde{F}_\alpha = K\bar{\rho}\left(\tilde{Y}^*_\alpha - \tilde{Y}_\alpha\right)/\Delta t$ applies a relaxation feedback to the Eulerian solver using the mean particle compositions ($\tilde{Y}^*_\alpha$). This term is used to enforce consistency between the redundant Eulerian fields and the mean particle quantities. Cleary et al. [5] have employed such a feedback in place of the chemical source term. In this work, this term is applied alongside the mean reaction rate so that its contribution is low compared to the other physical terms. Based on tests with a 1D non-premixed flame configuration, $K/\Delta t = 100s^{-1}$ showed reasonable consistency between Eulerian and Lagrangian solutions. For the temporal jet flame studied in this work, this value is much smaller than the inverse of the large-eddy turnover time ($\tau^{-1} = 30252s^{-1}$) (an important physical time scale). Increasing $K/\Delta t$ to the order of τ^{-1} did not affect the results presented here. For the WM simulations, $\tilde{F}_\alpha = 0$.

The viscous stresses are evaluated assuming Newtonian fluid properties while the heat and mass diffusion fluxes are calculated using Fourier's and Fick's laws respectively as discussed in Chen et al. [4]. The transport properties are computed using a mixture-averaged formulation.

The SGS stress tensor is evaluated using the artificial shear viscosity model while the SGS heat flux vector is evaluated using the artificial thermal conductivity model as discussed by Cook [6]. The implementation of the artificial fluid properties (AFP) in the current solver was validated on non-reacting configurations in [21]. The turbulent species diffusivities are evaluated from the artificial thermal conductivity based on the assumption of unity turbulent Lewis number.

Finally, the chemical source terms are closed using the WM or TPDF models as described in the following.

Well-mixed model

In the well-mixed model, the sub-grid TCI are neglected and the chemical source terms are directly evaluated from the filtered data on the LES grid, i.e.

$$\tilde{\dot{\omega}}_\alpha = \dot{\omega}_\alpha\left(\tilde{T}, \tilde{\mathbf{Y}}, \bar{P}\right). \tag{5}$$

TPDF model

In the TPDF model, the transport equation for the sub-grid joint probability density function of the composition variables (species mass fraction and internal energy) is solved using an equivalent Lagrangian system [13]. The particle evolution equations for position and composition are given as,

$$\mathbf{dx}^* = \left[\tilde{\mathbf{u}} + \frac{\nabla\left(\bar{\rho}\Gamma_{SGS}\right)}{\bar{\rho}}\right]^* dt + \sqrt{2\Gamma^*_{SGS}}\mathbf{dW}^*, \tag{6}$$

$$\begin{aligned} de^* = -\Omega_m\left(h^* - \tilde{h}^*\right)dt + \left[\frac{1}{\bar{\rho}}\nabla\cdot\mathbf{q^m}\right]^* dt \\ + \left[\frac{1}{\bar{\rho}}\left(\underline{\tau}:\underline{\mathbf{S}} - \bar{p}\nabla\cdot\tilde{\mathbf{u}}\right)\right]^* dt, \end{aligned} \tag{7}$$

$$dY^*_\alpha = -\Omega_m\left(Y^*_\alpha - \tilde{Y_\alpha}^*\right)dt + \left[\frac{1}{\bar{\rho}}\nabla\cdot\mathbf{J^m_\alpha}\right]^* dt + \left[\frac{1}{\bar{\rho}}\right]^* \dot{\omega}^*_\alpha dt, \tag{8}$$

where the superscript ϕ^* denotes a quantity (ϕ) at the particle position, $\tilde{\phi}^*$ denotes the mean (estimated on the Eulerian grid) interpolated to the particle position, $\mathbf{W}$ is the Weiner process, Γ_{SGS} is the turbulent diffusivity and $\underline{\mathbf{S}}$ is the strain-rate tensor.

The first term in the RHS of equations (7) and (8) represents SGS mixing that has been modelled with the IEM model [3]. The mixing frequency (Ω_m) is evaluated using $\Omega_m = C_\phi\left(\Gamma + \Gamma_{SGS}\right)/\Delta^2$ [13], where Δ is the grid spacing, Γ is the molecular diffusivity and C_ϕ is the mechanical-to-scalar mixing time-scale ratio taken as 2, unless specified otherwise [12]. The second term in the RHS of equations (7) and (8) represents the resolved drift terms where $\mathbf{q^m}$ and $\mathbf{J^m_\alpha}$ are the molecular heat flux and species mass diffusion flux respectively. This approach of including the resolved diffusion terms in the particle composition update has two advantages, firstly it avoids a spurious production term in the composition variance equation and secondly, it allows inclusion of differential diffusion in the particle transport [17]. The last term in the RHS of equation (7) represents the effects of compressibility and viscous dissipation on the particle internal energy. Finally, the chemical source term required in the Eulerian solver ($\tilde{\dot{\omega}}_\alpha$ in equation (3)) is taken as the mean reaction rate from the particle data, which is in a closed form with the TPDF approach (last term in the RHS of equation (8)).

Numerical schemes

High-order numerical schemes have been employed in the LES solver. The time integration is performed with an explicit six-stage, fourth-order Runge-Kutta (RK) algorithm [14], which is second-order accurate for the stochastic differential equation (equation (6)). The particle transport equations (6)-(8) are tightly coupled with the Eulerian governing equations (1)-(4) at every stage of the RK algorithm. The spatial derivatives are evaluated using an eighth-order accurate central difference scheme, with a cubic skew-symmetric treatment of the convective terms [15]. An eighth-order Padé-type tridiagonal filter [8] is applied after regular intervals (10 time steps) to suppress the high-frequency numerical errors.

Data on the mesh nodes is interpolated onto the particle positions using fourth-order Lagrange interpolation. The mean quantity ($\tilde{\phi}_j$) at a mesh node j is evaluated from the transported particle quantities (ϕ^*) as follows,

$$\tilde{\phi}_j = \frac{\Sigma K_j(x^*) m^* \phi^*}{\Sigma K_j(x^*) m^*}, \tag{9}$$

where, m^* and x^* are the particle mass and position respectively. $K_j(x^*)$ is the Kernel-weight defined as 1 if $|x_j - x^*| < \Delta_E$ and 0 otherwise. The Kernel width, Δ_E is taken as $\Delta/2$.

Particle number control algorithms are employed in order to maintain the particle count inside a finite difference cell within user specified bounds.

Configuration details

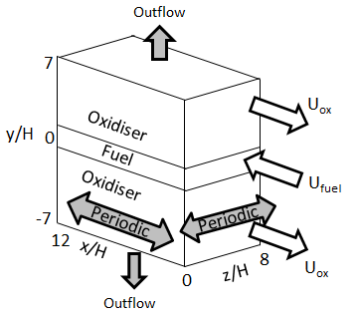

Figure 1: Schematic of the non-premixed temporal jet flame.

The schematic of the non-premixed temporal planar-jet flame is shown in Fig. 1. The fuel jet stream has an initial height

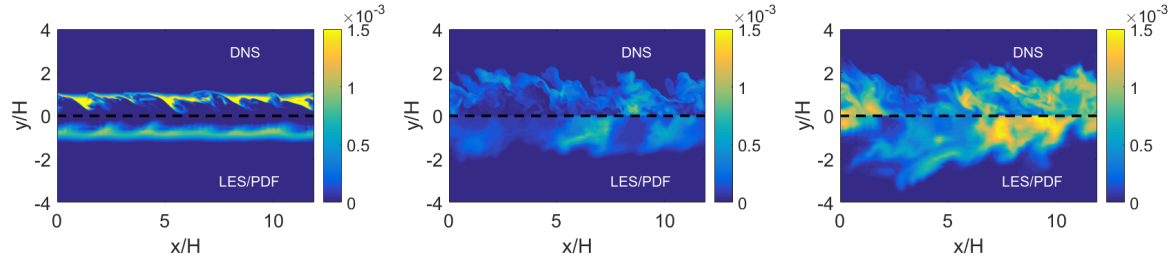

(a) $8t_j$ (b) $24t_j$ (c) $40t_j$

Figure 2: Contours of OH mass fraction on a x-y plane from DNS (upper half) and LES/PDF (lower half).

H = 1.37 mm and comprises of 50% CO, 10% H_2 and 40% N_2 by volume. The counter-flowing oxidiser stream has 25% O_2 and 75% N_2 by volume. A reduced chemical mechanism as discussed in [10] has been used in the current study. The jet Reynolds number based on H and the relative fuel velocity ($U_{fuel} - U_{ox}$) is 9079. The reader is referred to Hawkes et al. [10] for complete details of this configuration.

The domain size is 12H, 14H and 8H in the stream-wise(x), cross-stream(y) and the span-wise(z) directions respectively. The mesh employed in the DNS by Hawkes et al. [10] comprised of 72 points per H, which was 2× the size of the minimum Kolmogorov scales encountered. In the present LES, the grid size is taken as $\Delta = 9dx_{DNS}$, which corresponds to 8 points per H. A small time-step size of 5×10^{-8} seconds (acoustic CFL number of 0.1) is utilised for the simulations.

The LES simulations are initialised using first-order interpolation from the initial DNS dataset. For the LES/PDF simulation, the particles are randomly distributed in the Eulerian mesh and the initial composition variables are interpolated from the Eulerian data. The initial particle count in a cell (N_{pc}) is set to 30 and is bounded by $\{10, 60\}$ in the subsequent time-steps.

Results and discussion

The contours of OH mass fraction from the DNS and the mean particle data from the LES/PDF are shown for three jet times in Fig. 2. The contour at $8t_j$ is at the initial stage of the development of the temporal jet flame. The contours at $24t_j$ show significant flame extinction while by $40t_j$ the flame begins to re-ignite which has been qualitatively well captured with the LES/PDF simulation.

In order to quantitatively compare the LES results with the DNS, the statistics (mean and RMS) of mixture fraction (Z), temperature and OH mass fraction are compared. Figure 3 shows these statistics at three different jet times, namely $t_j = 8, 24$ and 40 for both the PDF and the well-mixed models. The statistics from the PDF simulation agree very well with the DNS results indicating that the flame extinction and re-ignition phenomena are well captured by this sub-grid model. On the other hand, the well-mixed approximation showed good agreement until the extinction stage, but significantly under-predicts the temperature and OH mass fraction at $40t_j$ implying that the flame re-ignition has not been captured by this model.

Figure 4 shows the mean temperature conditional on mixture fraction ($\langle T|Z \rangle$) at $40t_j$ from the DNS, LES/PDF for different values of mechanical-to-scalar time-scale ratio (C_ϕ) and the LES/WM simulation. The DNS study by Hawkes et al. evaluated C_ϕ to be approximately between 1.5 and 2 as a function of time for this configuration. In the current LES/PDF simulation, $C_\phi = 2$ gives excellent predictions of the flame re-ignition,

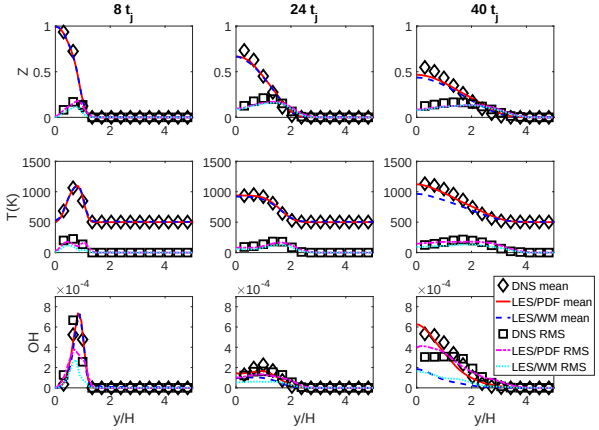

Figure 3: Mean and RMS profiles of mixture fraction, temperature and OH mass fraction from DNS, LES/WM and LES/PDF.

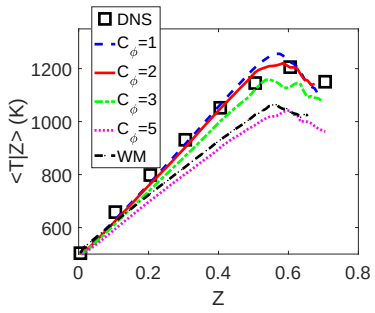

Figure 4: Temperature conditional on mixture fraction at $40t_j$ from DNS, LES/PDF for different values of C_ϕ and LES/WM

which is consistent with the estimate of C_ϕ from the DNS results. The sensitivity of these results in not significant for C_ϕ between 1 and 3 but increasing this parameter to 5 did not predict the flame re-ignition accurately. This result implies that if the sub-grid mixing is excessively large, the results tend towards the WM model predictions, which is as expected.

Conclusions

A temporally evolving non-premixed CO/H_2 jet flame involving significant extinction and re-ignition is simulated using a high-order compressible LES solver. Excellent predictions of the temperature and scalar statistics were demonstrated with the LES/PDF model on a coarse Eulerian grid. Further, the utility of the sub-grid TCI model was highlighted by comparing the results with a well-mixed approximation, which failed to predict

the flame re-ignition on the same Eulerian grid.

The LES/PDF results were noted to be dependent on the specification of the parameter C_ϕ which controls the sub-grid mixing frequency but showed low sensitivity about the value that was utilised in the current study ($C_\phi = 2$). In future, we aim to validate this solver on higher Reynolds and Mach number configurations.

Acknowledgements

This work was performed with funding support from the Australian Government Research Training Program Scholarship and the Australian Research Council (ARC). The research benefited from computational resources provided through the National Computational Merit Allocation Scheme, supported by the Australian Government. The computational facilities supporting this project included the Australian National Computational Infrastructure (NCI) National Facility (the partner share of the NCI National Facility provided by Intersect Australia Pvt. Ltd.) and the Pawsey Supercomputing Centre (with funding support from the Australian Government and the Government of Western Australia).

References

[1] Alhawwary, M. and Wang, Z., Fourier analysis and evaluation of DG, FD and compact difference methods for conservation laws, *J. Comput. Phys*, **373**, 2018, 835–862.

[2] Banaeizadeh, A., Li, Z. and Jaberi, F. A., Compressible scalar filtered mass density function model for high-speed turbulent flows, *AIAA Journal*, **49**, 2011, 2130–2143.

[3] Borghi, R., Turbulent combustion modelling, *Prog. Energy Combust. Sci.*, **14**, 1988, 245–292.

[4] Chen, J. H., Choudhary, A., de Supinski, B., DeVries, M., Hawkes, E. R., Klasky, S., Liao, W. K., Ma, K. L., Mellor-Crummey, J., Podhorszki, N., Sankaran, R., Shende, S. and Yoo, C. S., Terascale direct numerical simulations of turbulent combustion using S3D, *Comput. Sci. Discov.*, **2**.

[5] Cleary, M. J. and Klimenko, A. Y., A detailed quantitative analysis of sparse-Lagrangian filtered density function simulations in constant and variable density reacting jet flows, *Phys. Fluids*, **23**.

[6] Cook, A. W., Artificial fluid properties for large-eddy simulation of compressible turbulent mixing, *Phys. Fluids*, **19**, 2007, 1–9.

[7] Duwig, C., Nogenmyr, K.-j., Chan, C.-k. and Dunn, Matthew, J., Large eddy simulations of a piloted lean premix jet flame using finite-rate chemistry, *Combust. Theor. Model.*, **15**, 2011, 537–568.

[8] Gaitonde, D. V. and Visbal, M. R., Pade-type higher-order boundary filters for the Navier-Stokes equations, *AIAA Journal*, **38**, 2000, 2103–2112.

[9] Hawkes, E. R., Chatakonda, O., Kolla, H., Kerstein, A. R. and Chen, J. H., A petascale direct numerical simulation study of the modelling of flame wrinkling for large-eddy simulations in intense turbulence, *Combust. Flame*, **159**, 2012, 2690–2703.

[10] Hawkes, E. R., Sankaran, R., Sutherland, J. C. and Chen, J. H., Scalar mixing in direct numerical simulations of temporally evolving plane jet flames with skeletal CO/H2 kinetics, *Proc. Combust. Inst.*, **31**, 2007, 1633–1640.

[11] Haworth, D. C., Progress in probability density function methods for turbulent reacting flows, *Prog. Energy Combust. Sci.*, **36**, 2010, 168–259.

[12] Heinz, S., On Fokker–Planck equations for turbulent reacting flows . Part 2 . Filter density function for large eddy simulation, *Flow, Turbulence and Combustion*, **70**, 2003, 153–181.

[13] Jaberi, F. A., Colucci, P. J., James, S., Givi, P. and Pope, S. B., Filtered mass density function for large-eddy simulation of turbulent reacting flows, *J. Fluid Mech.*, **401**, 1999, 85–121.

[14] Kennedy, C. A. and Carpenter, M. H., Several new numerical methods for compressible shear-layer simulations, *Appl. Numer. Math.*, **14**, 1994, 397–433.

[15] Kennedy, C. A. and Gruber, A., Reduced aliasing formulations of the convective terms within the Navier – Stokes equations for a compressible fluid, *J. Comput. Phys*, **227**, 2008, 1676–1700.

[16] Klimenko, A. and Bilger, R. W., Conditional moment closure for turbulent combustion, *Prog. Energy Combust. Sci.*, **25**, 1999, 595–687.

[17] McDermott, R. and Pope, S. B., A particle formulation for treating differential diffusion in filtered density function methods, *J. Comput. Phys*, **226**, 2007, 947–993.

[18] Pitsch, H., Large-Eddy Simulation of Turbulent Combustion, *Annu. Rev. Fluid Mech.*, **38**, 2006, 453–482.

[19] Pitsch, H. and Steiner, H., Large-eddy simulation of a turbulent piloted methane/air diffusion flame (Sandia flame D), *Phys. Fluids*, **12**, 2000, 2541–2554.

[20] Raman, V., Fox, R. O. and Harvey, A. D., Hybrid finite-volume/transported PDF simulations of a partially premixed methane-air flame, *Combust. Flame*, **136**, 2004, 327–350.

[21] Ranadive, H. D., Wang, H. and Hawkes, E. R., Application of Artificial Fluid Properties for Stable and Accurate Large-eddy Simulations of Compressible Turbulent Reactive Flows, in *20th AFMC, Perth*, 2016.

[22] Wang, H., Popov, P. P. and Pope, S. B., Weak second-order splitting schemes for Lagrangian Monte Carlo particle methods for the composition PDF/FDF transport equations, *J. Comput. Phys*, **229**, 2010, 1852–1878.

[23] Wilkie, J., Numerical methods for stochastic differential equations, *Phys. Rev. E*, **70**, 2004, 017701.

[24] Wolf, P., Staffelbach, G., Roux, A., Gicquel, L., Poinsot, T. and Moureau, V., Massively parallel LES of azimuthal thermo-acoustic instabilities in annular gas turbines, *J. Phys. Conf. Ser*, **180**.

[25] Yang, Y., Wang, H., Pope, S. B. and Chen, J. H., Large-eddy simulation/probability density function modeling of a non-premixed CO/H2 temporally evolving jet flame, *Proc. Combust. Inst.*, **34**, 2013, 1241–1249.

[26] Zhang, L., Liang, J., Sun, M., Wang, H. and Yang, Y., An energy-consistency-preserving large eddy simulation-scalar filtered mass density function (LES-SFMDF) method for high-speed flows, *Combust. Theor. Model.*, **22**, 2018, 1–37.